Journal of Nuclear Materials 378 (2008) 1–8

Contents lists available at ScienceDirect

Journal of Nuclear Materials

journal homepage: www.elsevier.com/locate/jnucmat

Evidence of two gas release kinetics during the oxidation of an irradiated PWR UO_2 fuel

P. Menegon [a], L. Desgranges [b,*], Y. Pontillon [b,*], A. Poulesquen [c]

[a] Commissariat à l'Energie Atomique, CEA/Valrhô – Marcoule, DEN/DRCP/SE2A/LEHA, Bat. 166 – Atalante, BP 171 30207 Bagnols-sur-Cèze cedex, France
[b] Commissariat à l'Energie Atomique, Centre d'Etudes de Cadarache, DEN, Département d'Etude des Combustibles (DEC), Service d'Analyse et de Charactérisation du Comportement du Combustible (SA3C), 13108 Saint-Paul-lez-Durance cedex, France
[c] Commissariat à l'Energie Atomique, DEN/DPC/SECR, Centre d'Etudes de Saclay, Bat. 450 91191 Gif sur Yvette cedex, France

ARTICLE INFO

Article history:
Received 28 January 2008
Accepted 7 April 2008

ABSTRACT

The 'ADAGIO' (French acronym for Discriminating Analysis of Accumulation of Inter-granular and Occluded Gas) experiments are dedicated to the determination of the gas inventory located at inter-granular position thanks to a partial oxidation of an irradiated UO_2 fuel. During these experiments the ^{85}Kr gas release is measured as a function of time. The comparison of ^{85}Kr release kinetic with the fuel oxidation kinetic brought into prominence two different gas release kinetics: the first one is proportional to the oxidation kinetic, the second one has a sigmoid shape and could be linked to the gas release of the so called 'High Burn-up Structure'.

1. Introduction

The behaviour of fission gases is a key point for understanding and modelling irradiated nuclear fuel [1]. A specific attention is paid to the determination of the gas fraction which is trapped into bubbles, in particular at grain boundaries. This later population can indeed lead to grain boundary opening and significant gas release in off normal or accidental conditions [2]. Although a tremendous effort was performed in hot laboratories in order to improve both the measurement and local distribution of fission gases in the nuclear ceramics, only a few methods can provide quantitative information on the gas located at inter-granular position. Amongst them the 'ADAGIO' (French acronym for Discriminating Analysis of Accumulation of Inter-granular and Occluded Gas) method was developed at CEA (Commissariat à l'Energie Atomique) [3] in the wake of the pioneer Canadian team's work [4]. The global ADAGIO process is schematically described in Fig. 1. From a general point of view, this technique is based on the fact that fission gas inventory (intra- and inter-granular) can be distinguished by controlled fuel oxidation, since grain boundaries are oxidised under limited oxidation. In more details, typical PWR (Power Water Reactor) fuel samples – one pellet with its clad or a fraction of the pellet – is re-irradiated in a Material Testing Reactor (MTR) in order to create short half-life fission products distributed throughout the fuel matrix. The irradiation is performed at low temperature, to generate fission gases tracers located inside the grain, and under inert atmosphere in order to avoid any fuel oxidation. As a consequence, the comparison between the short half-life radioactive gases (for instance ^{133}Xe) and the long life ones (^{85}Kr), which concentration and location (within the grain, either in the sub-lattice or in bubbles, and at the grain boundaries in bubbles and as manufactured porosities) are not modified by the re-irradiation, allows to determine the fraction of gas located at the grain boundaries.

At the end of the re-irradiation the fuel rod is sent to the hot laboratory where annealing tests are performed. A first plateau at 450 °C (or 380 °C) under air flow is performed in order to induce the oxidation of UO_2 into $U_4O_{9\gamma}$ (called 'oxidation phase' throughout the paper). As this oxidation step occurs preferentially along the grain boundaries and due to the corresponding volume expansion (caused by UO_2 to $U_4O_{9\gamma}$ phase change) grain boundary separation occurs. As a consequence, the inter-granular gas is released and the potential intra-granular gas contribution is determined by the ^{133}Xe release. After this step, the temperature is increased in order to extract the remaining gas inventory. During all these operations, the ^{85}Kr and ^{133}Xe release are continuously monitored by the online gamma spectrometer (see below). These types of data will give information in order to go further in the development of more realistic and mechanistic modelling of FGR (Fission Gas Release) from fuels.

Recently the ADAGIO mathematical data treatment of the release kinetics, which allows an accurate determination of the ^{85}Kr release kinetics at the sample position, was improved. This made possible a new interpretation of the experimental data, evidencing two gas release kinetics during the so-called 'oxidation phase' of the global ADAGIO annealing test.

* Corresponding authors. Tel.: +33 (0)4 42 25 31 59; fax: +33 (0)4 42 25 44 79 (L. Desgranges.), tel.: +33 (0)4 42 25 72 26; fax: +33 (0)4 42 25 44 79 (Y. Pontillon).
E-mail addresses: lionel.desgranges@cea.fr (L. Desgranges), yves.pontillon@cea.fr (Y. Pontillon).

0022-3115/$ - see front matter © 2008 Elsevier B.V. All rights reserved.
doi:10.1016/j.jnucmat.2008.04.008

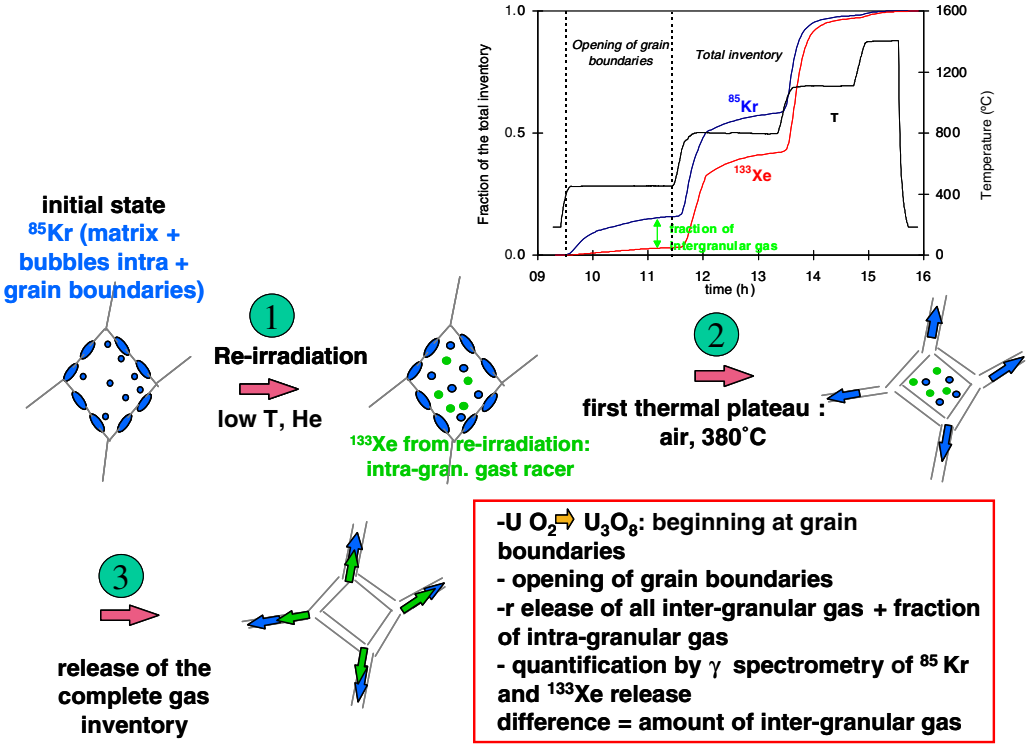

Fig. 1. Schematic description of the ADAGIO technique.

In this paper, after a brief description of the experimental setup, the mathematical treatment of the experimental ^{85}Kr release data will be presented and the obtained results discussed.

2. Experimental section

2.1. Annealing test facility

The whole annealing test facility, called MERARG (French acronym for Fission Gas Release Study Facility by Annealing) and depicted in Fig. 2, is settled in one of the hot cell laboratories (the LECA-STAR one) at Cadarache CEA center. This experimental set up has been described in details elsewhere [5]. As a consequence, only the key points will be recalled here. The corresponding key components are the induction furnace located in a shielded hot cell, the gamma spectrometry device, and the gloves box where gas coming out of the furnace is trapped.

The furnace chamber is a quartz tube; the sample is put into a crucible (Mo, W or Pt depending on the type of experiments) which is coupled to the high frequency (50 kHz) coil placed around the

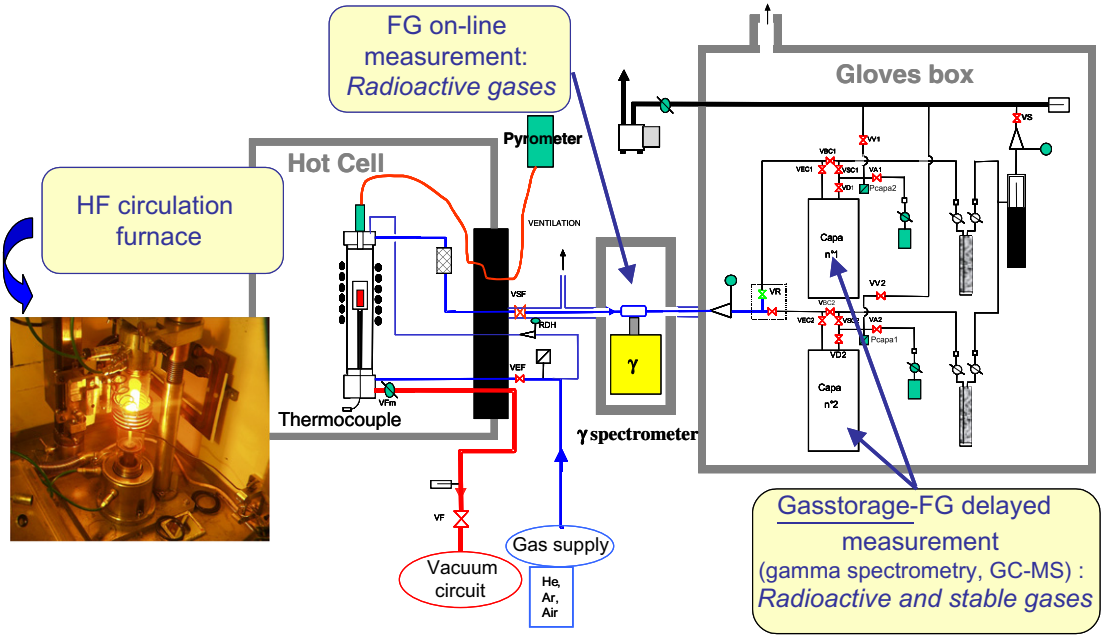

Fig. 2. MERARG annealing test facility.

quartz tube, and heated up by induction. During the whole annealing, the specimen is swept by a regulated gas flow (helium or air). Released fission gases are carried away with the sweeping gas; it flows through aerosol filters before passing in the delay chamber situated in front of the gamma spectrometer. The gas flow ends in the gloves box where fission gases are trapped.

The counting chamber and the detector are located in a shielded chamber. The aim of such measurements is to follow in a set and given point of an experimental loop, the evolution of the activity signal over time. The detector is a germanium P-type crystal. Radioactive fission gas activity is monitored by the gamma spectrometer. By taking into account fission gas dilution and flowing time between the furnace and the counting chamber, real fission gas release kinetics (i.e. at the sample position) can be reconstructed from the measured one (i.e. at the γ detector position) as detailed hereafter (Section 2.3).

Furnace temperature, gas flow and pressure are continuously monitored. The sample temperature is evaluated by two ways: (i) a thermocouple placed at the lower part of the crucible measures its temperature; (ii) a pyrometer gives another measurement for temperatures above 1000 °C by direct sighting into the sample chamber.

2.2. Sample characteristics

The main properties of the samples are displayed in Table 1. A slice was cut out of a UO_2 fuel rod irradiated 6 cycles (i.e. up to ~72 GWd/t_m) in a commercial PWR reactor operated by Electricité de France (EdF). The fuel rod pellets were manufactured by standard industrial process. The corresponding ^{235}U initial enrichment was 4.5%. The sample which was submitted to the annealing test included one fuel pellet with its cladding.

The so-called 'initial gas inventory', which corresponds to the initial fission product (FP) concentration inside the samples is obtained by a methodology based on both gamma spectrometry measurements and use of FP creation codes such as PEPIN or CESAR [6]. This value is used in order to calculate the released fractions from the measured instantaneous release during and at the end of the experiment.

The fractional fission gas release measured by a pin puncturing test after base irradiation was 5.8% of the initial gas inventory for the father rod (Table 1).

2.3. Real fission gas release kinetics reconstruction

The general FGR process can be schematized as depicted in Fig. 3, where $R(t)$, $N_c(t)$, $N_f(t)$ and N_{mes} are, respectively, the FGR at the sample position, the number of atom in the counting chamber at the moment t, the number of atom in the furnace at the moment t, and the number of atom as measured by the gamma station. V_f and V_c are the volume of the furnace and the counting chamber, respectively, and finally d the gas flow rate.

Table 1
Main properties of the sample used

Initial composition	UO_2
Burn-up	72 GWd/t_U
Released gas fraction during irradiation (measured)	5.8%
Released gas fraction during irradiation (calculated with METEOR code)	5.9%
Gas fraction at intergranular position (measured with ADAGIO method)	23.9%
Gas fraction at intergranular position (calculated by METEOR code)	23.0%
Rod average power (W/cm) cycle 1, 2, 3, 4, 5 and 6	155, 160, 180, 175, 145 and 160

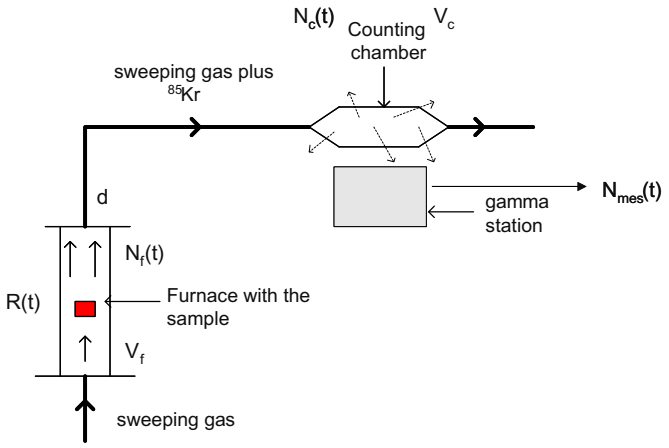

Fig. 3. FGR scheme (MERARG facility).

As explained above, the main objective of this procedure is to express the real fission gas release kinetics (i.e. at the sample position) from the measured one by taking into account fission gas dilution and flowing time between the furnace and the counting chamber. In other words, one has to express $R(t)$ as a function of $N_{mes}(t)$.

The ^{85}Kr balance, in number of atoms, at the furnace exit at moment t is given by

$$\frac{dN_f}{dt}(t) = R(t) - \frac{d}{V_f}N_f(t). \quad (1)$$

Beside, the same balance but between the furnace entrance and exit is given by (Eq. (2)).

$$\frac{dN_c}{dt}(t) = \frac{d}{V_f}N_f(t) - \frac{d}{V_c}N_c(t). \quad (2)$$

While applying the Laplace transform to Eqs. (1) and (2), one obtains (with $N_f(t=0) = N_c(t=0) = 0$ as initial condition):

$$s\bar{N}_f(s) = \bar{R}(s) - \frac{d}{V_f}\bar{N}_f(s), \quad (3)$$

$$s\bar{N}_c(s) = \frac{d}{V_f}\bar{N}_f(s) - \frac{d}{V_c}\bar{N}_c(s). \quad (4)$$

From these two latter equations, it is possible to express R as follows:

$$\bar{R}(s) = \left(\frac{V_f}{d}s^2 + \left[\frac{V_f}{V_c} + 1\right]s + \frac{d}{V_c}\right)\bar{N}_c(s), \quad (5)$$

which allows to express $R(t)$ as a function of $N_c(t)$ while applying the inverse Laplace transform (Eq. (6)) (with $N_c = 0$, $\frac{dN_c}{dt} = 0$ at $t = 0$):

$$R(t) = \frac{V_f}{d}\frac{d^2N_c}{dt^2}(t) + \left(1 + \frac{V_f}{V_c}\right)\frac{dN_c}{dt}(t) + \frac{d}{V_c}N_c(t). \quad (6)$$

At this stage, it is important to note that the measurement does not allow to access directly to the expression of the $N_c(t)$ function. In fact, between a time interval t_i and t_{i+1}, which corresponds to the counting time of one gamma spectrum, the number of atoms measured by the detector is given by[1]

$$N_{mes}\left(\frac{t_i + t_{i+1}}{2}\right) = \frac{1}{t_{i+1} - t_i} \times \frac{V}{V_c} \times \int_{t_i}^{t_{i+1}} N_c(\tau)d\tau. \quad (7)$$

But, if we consider that $N_c(t)$ is more or less constant between t_i and t_{i+1} and equal to its value at the middle of the interval (Eq. (7)) becomes

[1] If one affects the measurement performed during $[t_i; t_{i+1}]$ to the moment $(t_i + t_{i+1})/2$ and with V corresponding to the 'seen' by the gamma detector.

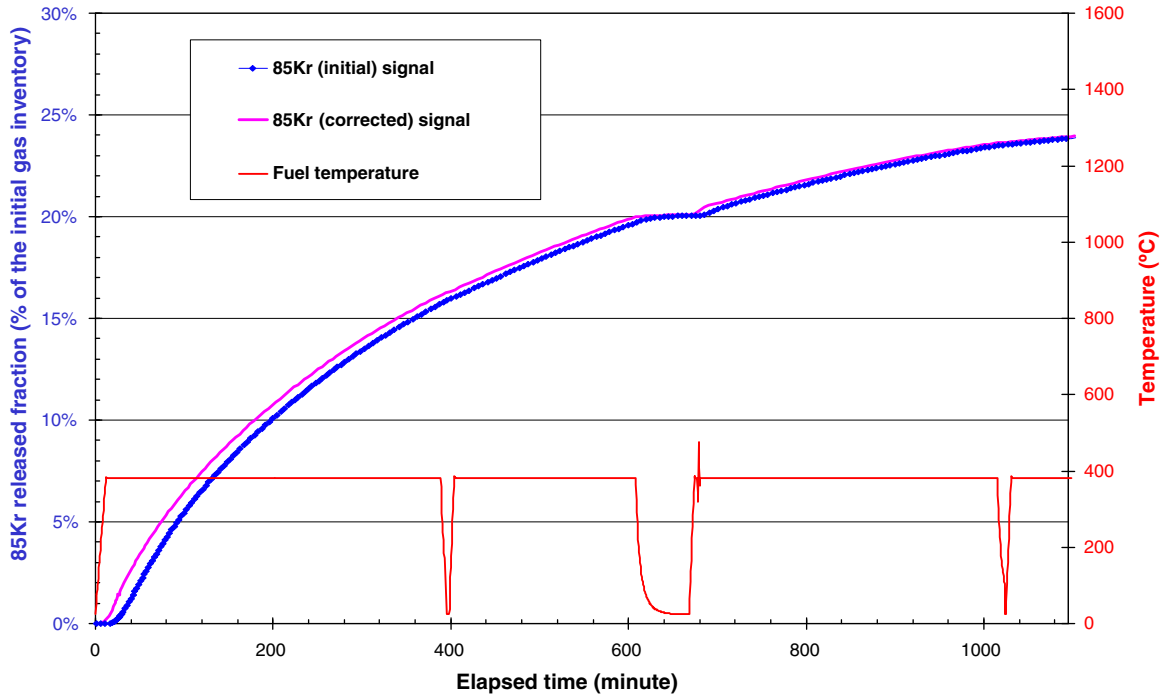

Fig. 4. Sample temperature profile together with the corresponding ^{85}Kr release rate as a function of time: Cumulated release. The curve in blue corresponds to the initial signal (i.e. at the detector position). The curve in pink corresponds to the corrected signal (i.e. at the sample position) calculated according to the procedure described in Section 3). (For interpretation of the references to colour in this figure legend, the reader is referred to the web version of this article.)

$$N_c\left(\frac{t_i+t_{i+1}}{2}\right)=\frac{V_c}{V}\times N_{mes}\left(\frac{t_i+t_{i+1}}{2}\right). \tag{8}$$

As a consequence, it is possible to calculate the first and second derived of $N_c(t)$ (Eqs. (9) and (10), respectively) by using a development in Taylor series.

$$\frac{dN_c}{dt}(t_j)=\frac{N_c(t_{j+1})-N_c(t_{j-1})}{t_{j+1}-t_{j-1}}, \tag{9}$$

$$\frac{d^2N_c}{dt^2}(t_j)=\frac{2}{t_{j+1}+t_{j-1}}\times\left(\frac{N_c(t_{j-1})}{t_j-t_{j-1}}+\frac{N_c(t_{j+1})}{t_{j+1}-t_j}-\left(\frac{1}{t_j-t_{j-1}}+\frac{1}{t_{j+1}-t_j}\right)\times N_c(t_j)\right). \tag{10}$$

That allows to express $R(t)$, (Eq. (6)), as a function of $N_{mes}(t)$ by combining (Eqs. (8)–(10)).

2.4. Thermal history applied to the sample

The sample was first submitted to a 18 h long annealing treatment at 380 °C under dry and refurbished air supplied by Air Product©. For technical reason,[2] this annealing was performed in 4 cycles of approximately 400, 200, 400, 60 min each. It corresponds to the 'oxidation phase' of the global ADAGIO process. The temperature profile is presented, together with the experimental cumulated ^{85}Kr releases measured at the detector position, as a function of time in Fig. 4.

2.5. Numerical treatment of the oxidation kinetics

The ^{85}Kr release observed in our experiment is a consequence of the UO_2 ceramic oxidation. The experimental conditions have been chosen in order to avoid the formation of U_3O_8 into the bulk which would have induced intra-granular cracking. As a consequence the oxidation proceeded from irradiated UO_2 to $U_4O_9\gamma$ as reported by Thomas et al. [7].

In literature, the kinetic of this reaction is reproduced by the Janders equation [8,9] (although this equation is not fully justified [10]):

$$\alpha=\left[1-(1-\sqrt{\kappa t})^3\right], \tag{11}$$

where α is the ratio of the molar number of formed $U_4O_9\gamma$ to that of the initial UO_2, t is time and κ is a constant related to the grain size and the oxygen diffusion with the formula:

$$\kappa=\frac{k}{(r*a)^2}, \tag{12}$$

where r is the radius of the UO_2 original grain considered as a sphere, a is the ratio of the molar volume of the product to that of the starting material (here a is close to 0.98) and k is the diffusion controlled rate constant.

Although this equation may be well suited to reproduce the weight gain measured during the oxidation of un-irradiated UO_2 powder, its fitting is poorer with the weight gain data obtained with irradiated fuel, especially for the low oxidation rates. Jander's equation induces indeed an infinitive derivative at $t=0$, which is not observed for irradiated fuel. In order to overcome this difficulty, the Jander equation was modified as follows:

$$\alpha=\exp\left(\frac{-1}{B*t}\right)*\left[1-(1-\sqrt{\kappa t})^3\right]. \tag{13}$$

The added term modifies the curve only for the lower oxidation rates, and allows to take into account the 'incubation' period observed in experiments performed on irradiated samples (sigmoid shape of weight grain curve). This modified equation (Eq. (13)) was used successfully in order to reproduce the oxidation kinetic on several published weight gain data sets. Fig. 5 presents the weight curves obtained on a UOX used fuel oxidised at 200 °C dur-

[2] Particularly because the annealing has had to be stopped according to particular laboratory regulation during these experiments.

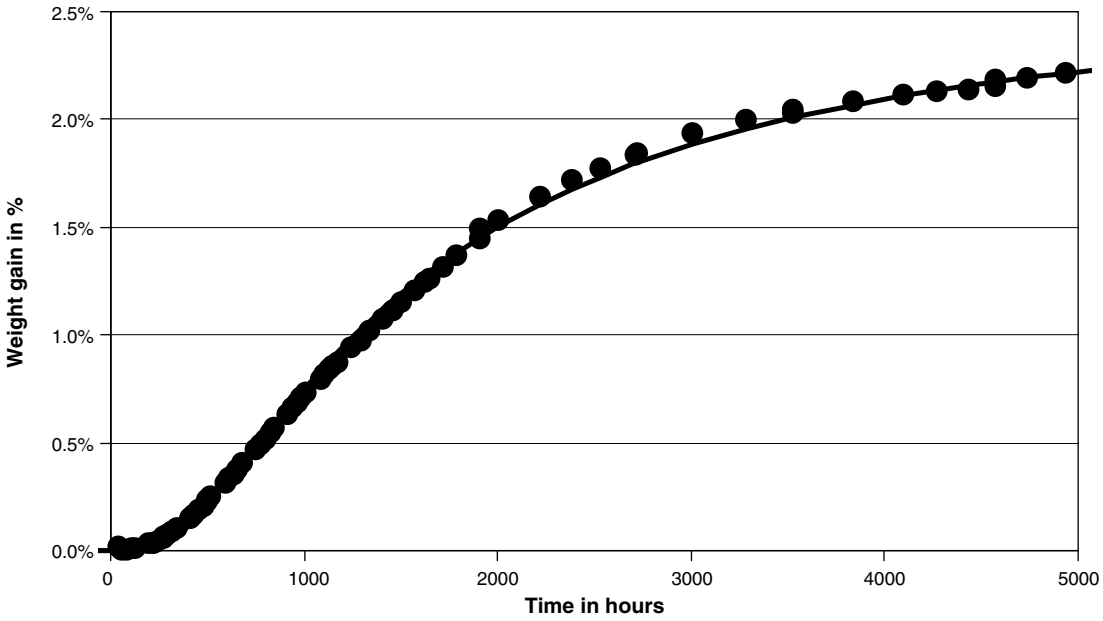

Fig. 5. Comparison between experimental irradiated UO_2 oxidation weight gain data [11] and the modeling given by Eq. (13).

ing 5000 h, taken from [11], and the curve obtained with the modified Janders' law taking B and κ equal to 2.5×10^{-7} s^{-1} and 5×10^{-8} s^{-1}. The agreement was rather good and, taking a 5 μm radius for the UO_2 grains, it gives k value equal to 10^{-19} m^2 s^{-1}, consistent with [8]. However it is clear that the modified Jander equation has no explicit physical meaning, anyhow it allows a good reproduction of the weight gain curve, which is the objective sought in this study.

3. Gas inventory

The ADAGIO technique was initially devoted to the determination of the gas inventory, especially at inter-granular position. In this part, the quantitative data obtained with ADDAGIO method using the sample presented above are detailed.

3.1. Release data

The ^{85}Kr initial signal was treated with the mathematical treatment explained previously. The resulting curves, corresponding to the real ^{85}Kr release kinetics at the sample position, are also presented in Fig. 4. After this first stage, the temperature has been increased up to 1500 °C by successive steps under air in order to extract all the fission gases located inside the sample. The released gas fraction at the end of the oxidation phase (T = 380 °C) is determined to be 23.9%, while the total released fraction of gas at the end of the experiment is equal to 94.2%.

As far as the cumulated release is concerned, the ^{85}Kr kinetics can be divided into two main stages: (1) from 0 to 150 min, where the release curve has a parabolic shape, and (2) from 150 min to the end of the test, where the release curve is approximately linear.

3.2. Gas inventory consistency

In previous studies [12], a sample re-irradiation in a research reactor was performed before the experiment in order to estimate the gas fraction coming from the grain bulk. During the first annealing step, ^{133}Xe and ^{85}Kr were simultaneously measured, since during the re-irradiation short half-life radioactive gas, ^{133}Xe, is re-created in intra-granular position and is considered as a good tracer of the global intra-granular gases. Anyhow, it was shown that the gas coming from the bulk represents only a small fraction of the total released quantity during ADAGIO oxidation (typically 1–1.5% of the initial gas inventory). As a consequence, in our experiment only the ^{85}Kr release was measured.

The total cumulated release obtained by ADAGIO ((94.2 ± 9.5)%) is in good agreement with the release measured by pin puncturing test after base irradiation ((5.8 ± 0.4)%). Consequently, it appears that the calculated value of the initial gas inventory fit rather well with the experimental one. Therefore, the inter-granular gas fraction, which is the ratio between the experimental cumulated release and the experimental initial gas inventory, does not include artefacts due to the evaluation of the initial gas inventory. Besides, the global inter-granular gas population and the release after the base irradiation was also determined by the CEA fuel performance code METEOR [13]. These calculated results are in good agreement both with the ADAGIO measurement (23.9% of inter-granular gas measured instead of 23.0% calculated by METEOR, Table 1) and the pin puncturing test (5.9% for calculations to be compared to 5.8% for experiments). In conclusion, it can be stated that the experiment yielded accurate evaluation of the global inter-granular gas fraction ('classical' inter-granular bubbles and High Burn-up Structure (HBS) ones) without, as expected, too much contribution of the intra-granular gas, which was not characterized in this experiment.

4. Gas release kinetics

The new data treatment presented in this paper permitted the first accurate determination of inter-granular gas release kinetics at the sample position in the oxidation phase of the ADAGIO technique. In this part, this kinetics is discussed.

Grain boundary behaviour was interpreted by MacEachern [8], who stated that 'Used LWR fuel sample have rapid grain-boundary oxidation, so that oxidation proceeds in such samples much like oxidation of a powder sample having particle size equal to the grain size of the used fuel'. Thomas et al. [7] detailed this assumption, with TEM observations, saying: 'Rapid oxidation along the grain boundaries in spent fuel is attributed to rapid diffusion of

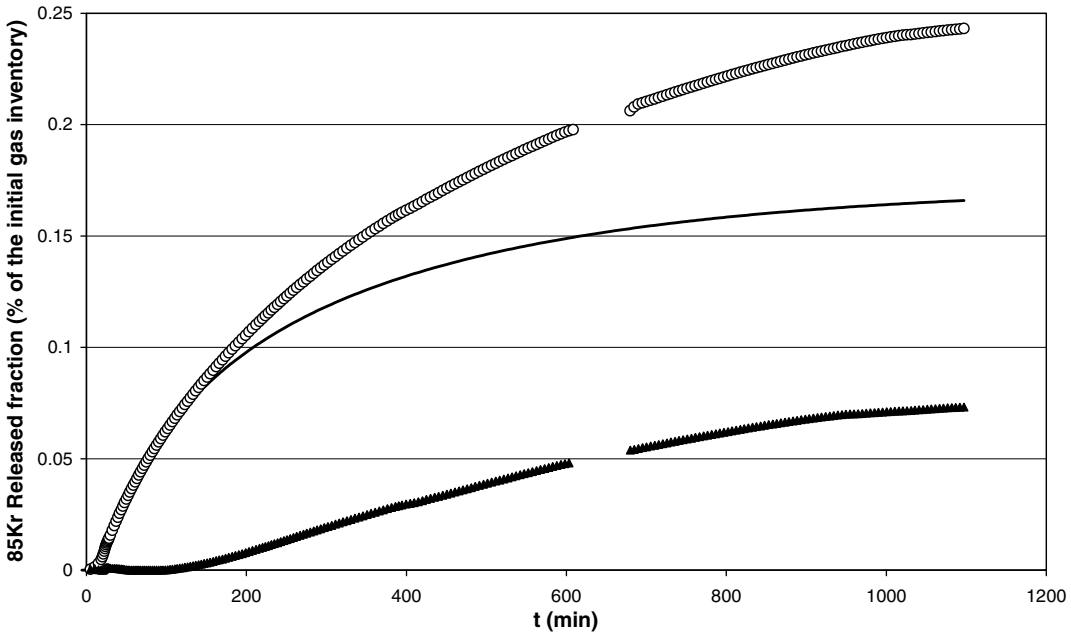

Fig. 6. ^{85}Kr release curve (open circle), fitted curve with the modified Jander's equation (straight line) difference between these two curves (plain triangle)

oxygen through the small (1–10 nm) closely spaced gas bubbles along the grain boundaries'.

If the gas filling these inter-granular bubbles is assumed to diffuse like oxygen molecules, the inter-granular gas release would then consist in a rapid burst at the beginning of the oxidation. Our experimental results do not agree with such hypothesis. On the contrary, the parabolic shape observed on Fig. 4 has some similarity with the oxidation weight gain curve of Fig. 5. In order to check this similarity, the ^{85}Kr release curve was compared with modified Janders' equation.

4.1. Data treatment

In order to apply modified Janders' equation to fission gas release, α_F is used in Eq. (13) instead of α. α_F is equal to the ratio of the measured ^{85}Kr release to a given amount, G, which would correspond to the total release obtained after complete oxidation into $U_4O_9\gamma$.

Adjusting B, κ and G to 0.025 min^{-1}, 5×10^{-4} min^{-1} and 18%, respectively, it was possible to draw α_F as a function of time and to compare it to the ^{85}Kr release curve; both curves are given in Fig. 6. The agreement between the two curves is very satisfactory up to approximately 150 min. Above 150 min α_F does not reproduce the total release. It appears that the difference between the two curves has a sigmoid shape as a function of time from 150 to 800 mn, where the instantaneous ^{85}Kr release tends to zero. Hence the ^{85}Kr release can be reproduced by the sum of two curves: a first one reproducing the oxidation kinetics of the irradiated UO_2 ceramic, and the other starting at approximately 150 min and being more or less linear with time.

The two release kinetics will be discussed separately.

4.2. First oxidation kinetics

The first ^{85}Kr release kinetic is described by the modified Jander's equation.

The Janders' equation implicitly admit that a discrete surface layer of U_4O_9/U_3O_7 forms on UO_2, but similar curves can be obtained taking into account a oxygen concentration gradient [8]. For the sake of simplicity, we consider that the modified Janders' equation describes the propagation of an oxidation front within the solid, whatever the exact nature of this front.

The correlation between Janders' equation and the inter-granular gas release suggests that the gas release occurs during the oxidation front propagation. Considering the oxidation front inside the UO_2 grains is not consistent with our results as said before. Our results are better understood by assuming that this oxidation front occurs inside ceramic fragments. The existence of oxidation front inside fragments was observed in [14] and [15] for example. Thus the gas release could be associated to the oxidation front, in

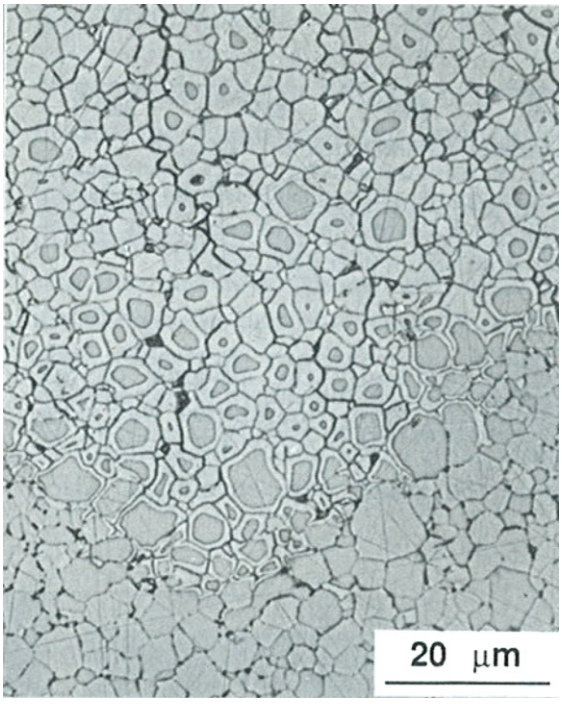

Fig. 7. Evidence of an oxidation propagation front inside an irradiated fuel fragment from [15].

which grain boundaries could be opened. The formation inter-granular cracks associated to $U_4O_9\gamma$ formation [15] is consistent with this interpretation (Fig. 7). This assumption is also consistent with the fact that the oxidation weight gain data do not exactly obey the true Janders' equation, the experimental shape would be due to the complex kinetics of the oxidation front, which would include both grain boundaries and bulk oxidation kinetics. Moreover, using κ value determined by the fitting with the modified Jander's equation, the value of k obtained for a fragment size ($r = 100\ \mu m$), equal to $5 \times 10^{-16}\ m^2\ s^{-1}$, is in better agreement with the values reported by MacEachern, ranging from 3×10^{-16} to $7 \times 10^{-16}\ m^2\ s^{-1}$, than the k value determined for a grain size ($r = 6\ \mu m$) equal to $1.8 \times 10^{-18}\ m^2\ s^{-1}$. Finally G has a value of approximately 18% which is consistent with other estimation of the gas inventory on grain boundaries for that type of fuel (HBS excluded).

4.3. Second oxidation kinetics

The existence of an additional gas release, with a sigmoid shape, could originate from the so called 'rim', or more properly named the High Burn-up Structure (HBS). HBS is known to occur when local burn-up exceeds 60–70 GWd/t_U. In our sample it affects a ring, approximately 80–100 μm wide (see Fig. 8), at the pellet periphery. This represents only ~5% of the mass of the pellet, but around ¼ of the inter-granular gas of the sample (evaluated from [16]). This huge amount of inter-granular gas results from a change in the ceramic microstructure associated to the HBS, in which 10–20% porosity is created by the formation of bubbles of the micrometer size. Its quantity of gas and its small influence on weight gain curve make it possible for the HBS to be responsible of the additional gas release.

This hypothesis is also consistent with the kinetic of this additional gas release. Because our sample has a high burn-up, the gap between the fuel pellet and the cladding is closed prohibiting the direct access of oxygen to HBS. Thus, oxygen must first diffuse through the ceramic fragment to reach the HBS. This can explain why the additional gas release is not observed at once, but only after an incubation time. Moreover, HBS contains a non negligible part of actinide and lanthanide compound, which are known to slow down the oxidation kinetics [9]. If it was assumed that the gas was released proportionally to the oxygen up take of HBS,

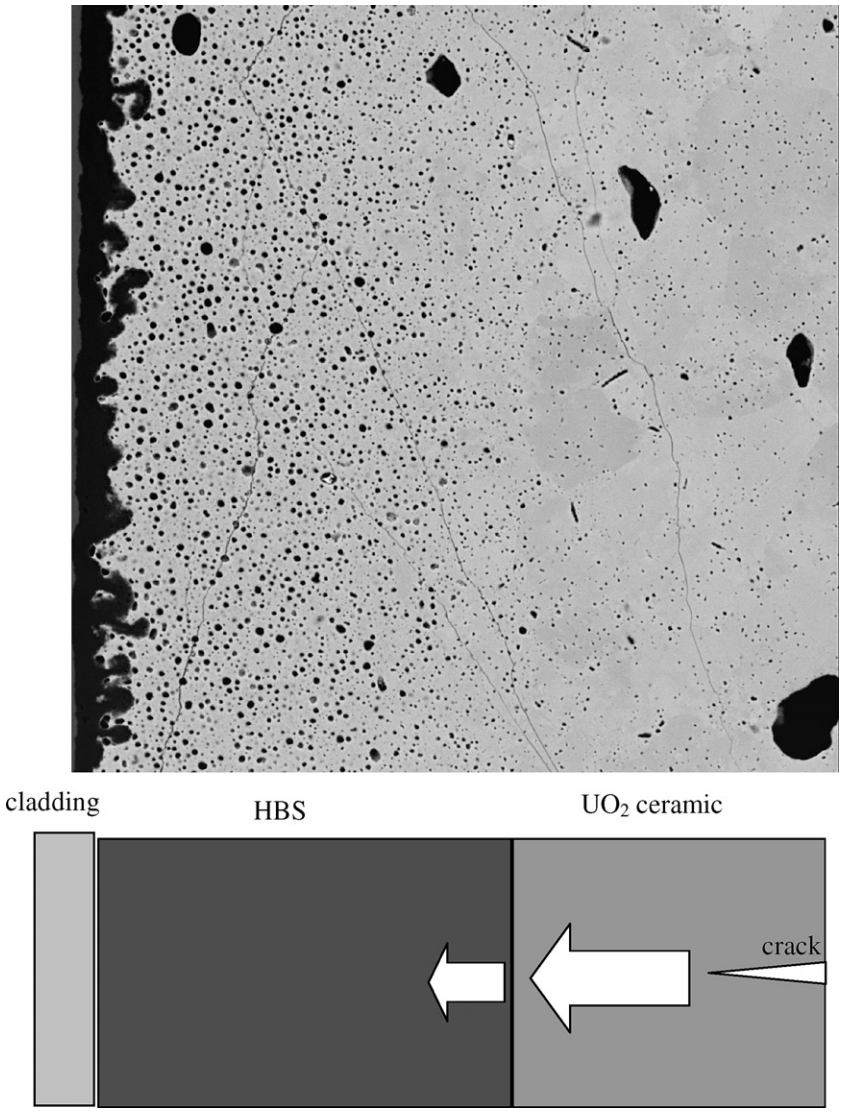

Fig. 8. SEM image ($166 \times 166\ \mu m^2$) of the RIM area associated to a scheme showing how the HBS structure can be oxidised. The white arrow represents the oxygen diffusion through UO_2 fragment and HBS (see text for details).

the linear part of the sigmoid kinetic could be explained by a constant oxygen flux into HBS, resulting from the diffusion of oxygen through the ceramic fragment to reach HBS.

5. Conclusion

The ^{85}Kr release data treatment improvement allowed determining the release kinetic at the sample position. The results obtained with a 6 cycles irradiated UO_2 sample evidenced two release kinetics. These kinetics were attributed to the inter-granular bubbles and the HBS bubbles. This new results opens the path to improved characterisation of the gas inventory inside irradiated nuclear fuel. Anyhow, the interpretation given here has to be validated on more numerous samples, in order to create a database.

Acknowledgements

The authors are indebted to Electricité de France for its financial support. They also wish to thanks J. Piquemal, M. Pontillon, G. Volle for their contribution to MERAG experimental work.

References

[1] M. Lippens, D. Boulanger, L. Mertens, in: Proceedings of NEA Seminar on Fission Gas behaviour in Water Reactor Fuels, 26–29 September 2000, Cadarache, France
[2] F. Lemoine, in: Proceedings of the 2005 Water Reactor Fuel Performance Meeting, October 2–6, 2005, Kyoto, Japan
[3] (a) S. Ravel, G. Eminet, E. Muller, L. Caillot, in: Proceedings of the Fission Gas Behaviour in Water Reactor Fuels, Nuclear Science OECD NEA, OECD, Cadarache, France, 2000, p. 347.;
(b) Y. Pontillon, J. Noirot, L. Caillot, E. Muller, in: 2007 International LWR Fuel Performance Meeting, San Francisco, California, September 30–October 3, 2007.
[4] (a) C.E.L. Hunt, F.C. Iglesias, D.S. Cox, N.A. Keller, R.D. Barrand, R.F. O'Connor, J.R. Mitchel, G.W. Wood, R. Miksusch, in: CNS 10th Annual Conference, June 1989. Also as report AECL-10036.;
(b) P.H. Elder, D.S. Cox, L.W. Wilkinson, R.V. Murphy, in: CNS 10th Annual Conference, June 1989. Also as report AECL-10036.
[5] (a) Y. Pontillon, J. Bonnin, et al. in: European Working Group, Hot Laboratories and Remote Handling, Plenary Meeting, Petten, the Netherlands, May, 2005 23rd–25th, 2005.;
(b) Y. Pontillon et al., in: 2005 Water Reactor Fuel Performance Meeting, October 2–6, 2005, Kyoto, Japan.
[6] Y. Pontillon, G. Ducros, et al., in: International Conference, Nuclear Energy for New Europe 2006, Portorož, Slovenia, September 18–21, 2006.
[7] L.E. Thomas, R.E. Einziger, R.E. Woddley, J. Nucl. Mater. 166 (1989) 243.
[8] R.J. McEachern, J. Nucl. Mater. 245 (1997) 238.
[9] R.J. McEachern, P. Taylor, J. Nucl. Mater. 254 (1998) 87.
[10] G. Rousseau, L. Desgranges, F. Charlot, N. Millot, J.C. Nièpce, M. Pijolat, F. Valdivieso, G. Baldinozzi, J.F. Bérar, J. Nucl Mater. 355 (2006) 10.
[11] Lionel Desgranges, Gurvan Rousseau, Marie-Pierre Ferroud-Plattet, Cécile Ferry, Hélène Giaccalone, Isabelle Aubrun, Pierre Delion, Jean-Michel Untrau, in: P. Van Isheghem (Ed.), Scientific Basis for Nuclear Waste Management XXIX, Mater. Res. Soc. Symp. Proc., vol. 932, Warrendale, PA, 2006, paper no 18.
[12] Y. Pontillon, M.P. Ferroud-Plattet, et al. Experimental and Theoretical Investigation of Fission Gas Release from UO_2 up to 70 GWd/t under Simulated LOCA Type Conditions: The GASPARD Program, in: Proceedings of the 2004 Water Reactor Fuel Performance Meeting, September 19–24, 2004, Orlando, Floride, USA.
[13] C. Struzik, M. Moyne, J.P. Piron, 1997, in: Proceedings of ANS Conference, Portland, Oregon.
[14] K.M. Wasywich, W.H. Hocking, D.W. Shoesmith, P. Taylor, Nucl. Technol. 104 (1993) 309.
[15] L.E. Thomas, R.E. Einziger, R.E. Woodley, J. Nucl. Mater. 166 (1989) 243.
[16] J. Noirot, L. Noirot, L. Desgranges, J. Lamontagne, Th. Blay, B. Pasquet, E. Muller, Fission Gas Inventory in PWR High Burnup Fuel: Experimental Characterization and Modeling, in: Proceedings of the 2004 International Meeting on LWR Fuel Performance, Orlando, Florida, September 19–22, 2004.